

The inversion of the Equatorial Undercurrent in the western tropical Pacific during 1986/1987 El Niño event

Wang Zongshan,¹Jin Meibing,¹Zou Emei¹ and Xu Bochang¹

(Received November 14, 1992; accepted January 15, 1993)

Abstract— On the basis of time series measurements of winds, currents, temperature and salinity from equatorial current meter mooring and acoustic Doppler current profiler during the PRC/USA joint air-sea interaction studies in the western tropical Pacific Ocean and sea level data provided by Prof. Wyrki, analyses are made of the physical process and mechanism for the exceptionally inverse phenomenon (westward) of the Equatorial Undercurrent (EUC) in the western tropical Pacific after entering the mature stage of 1986/1987 ENSO event, and the numerical simulation is also conducted by "cross section" model. The results indicate that the inversion of the EUC is related to that of pressure gradient force near the equator under the influence of non-local permanent westerlies.

INTRODUCTION

The Equatorial Undercurrent (EUC) in the Pacific (also known as Cromwell) is an ocean current which lies in the thermocline near the equator and traverses the ocean basin from west to east. It originates from the deep layer west of 136.5° E at the depth deeper than 500 m, flows afterwards eastward, and rises sharply to about 250 m near 137° E, then gradually approaches sea surface in the equatorial eastern Pacific, its current width is about 400 km and lies on about 200 m layer (Halpern, 1983; State Oceanic Administration, 1981). The volume transport range of the EUC in the western and mid-Pacific varies from $10 \times 10^6 \text{ m}^3/\text{s}$ to $80 \times 10^6 \text{ m}^3/\text{s}$, the mean EUC transport is $41 \times 10^6 \text{ m}^3/\text{s}$ (Picaut and Tournier, 1988), the EUC is one of the salient dynamic factor in transporting warm water in the tropical western Pacific to the east.

Since the EUC at the equator south of Hawaii was discovered by H. N. Smith in September 1951, many oceanographers have paid more attention to observation and theoretical study of the EUC in the Pacific. During the period of the 1950s and the 1960s, scientists laid emphasis on exploring the EUC structure and its response to eastward tradewinds; from the beginning of the 1970s, they put the stress on the variability of the EUC and focused on the generation and decline of the equatorial current system including the EUC (Philander, 1980). So far, the mechanism

1. First Institute of Oceanography, State Oceanic Administration, Qingdao 266003, China

for the EUC formation has been exposed clearly, the result of numerical simulation is consistent with the measurement, i. e., in the tropical area, intense eastward tradewinds produce zonal sea level slope and eastward pressure gradient force, thus inducing equatorward meridional circulation in both Hemispheres, and the Coriolis tends to be zero at the equator, pressure gradient leads to the eastward flowing of momentum, so that the eastward advection is formed in the subsurface—the EUC; in the meantime, there is a westward South Equatorial Current (SEC) caused by westward momentum under easterlies in ocean Ekman layer (Charney, 1960; Gill, 1982; Halpern, 1987; McCreary, 1981; McPhaden *et al.*, 1990; Philander, 1980; Philander and Pacanowski, 1980). It is indicated that the formation of the EUC is closely associated with eastward tradewinds and pressure gradient force.

However, during the ENSO events, tradewinds collapse; westerlies burst; spikes of sea level move eastward; the volume transport of the EUC decreases (Gill, 1982; Picat and Tournier, 1988; Wang and Zou, 1987), and Firing *et al.* (1983) found that the upper and middle parts of the EUC disappeared at $0^{\circ}, 159^{\circ} \text{W}$, and the westward current (from the end of August to that of October 1982) and the strongest eastward jet (from the middle of October to the end of December) occurred near the surface during 1982/1983 ENSO event. Moreover, Guan (1986) discovered that the EUC completely disappeared and there existed a westward current between $0.5^{\circ} \sim 1.5^{\circ} \text{N}$ at 137°E from the beginning of July 1982, two months before the 1982/1983 ENSO event, after the large scale equatorial westerlies ($130^{\circ} \sim 160^{\circ} \text{E}$) prevailed. Later, Halpern (1983, 1987) also observed the same phenomenon. During the third cruise (September - October 1987) of PRC/USA joint air-sea interaction studies in the tropical western Pacific, we clearly observed the evidence of the EUC flowing reversely in the tropical western Pacific. However, the mechanism of such anomalous phenomenon still remains unknown. In this paper, in order to reveal the formation mechanism of the anomalous phenomenon, the authors first try to make qualitative analysis using measured data, then construct a numerical model by means of "cross section" model.

REVERSION OF THE EUC

Figure 1 shows time series of meridional velocity at 165°E for the period of October 13~21, 1987 measured from acoustic Doppler current profiler (ADCP). It is seen from Fig. 1 that although there was weak eastward current in 75 m layer, westward current prevailed from surface down to 350 m, the core of the EUC lay on about 200 m with typical speed of $-30 \sim -40 \text{ cm/s}$, the Equatorial Intermediate Current (EIC) situated below the EUC considerably strengthened with maximum speed of -40 cm/s and widened ($3^{\circ} \text{S} \sim 2^{\circ} \text{N}$). The time series of zonal velocity observed from current meter mooring ($0^{\circ}, 165^{\circ} \text{E}$) (see Fig. 2) showed that the EIC began to rise up from the middle of July 1987 and merged into the reverse EUC during the middle of September - the beginning of November, the surface occupied by eastward flowing current (shallower than 100 m) also switched to westward current from the middle of October to the end of November. During the EUC reversion, the responds of the current shallower than middle layer to the

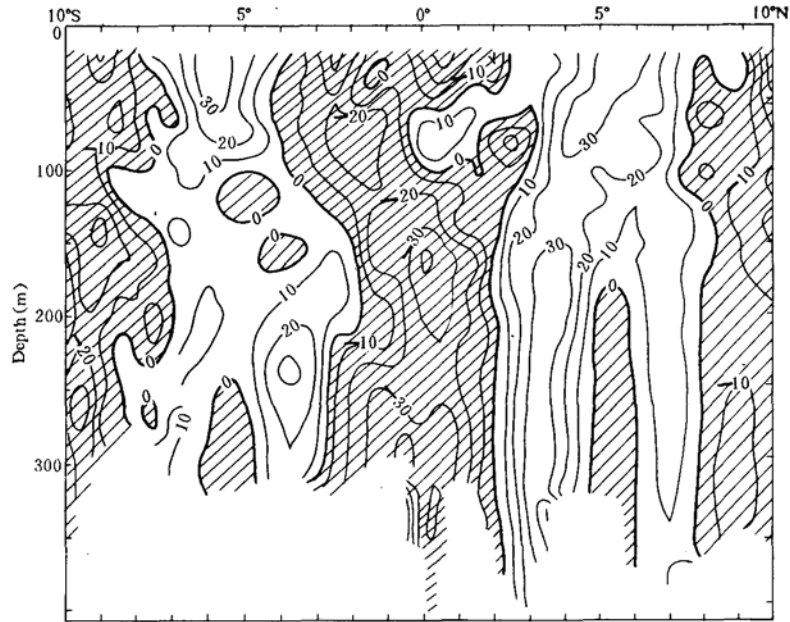


Fig. 1. Zonal component of velocity along 165° E section measured by ADCP (October 13~21, 1987).

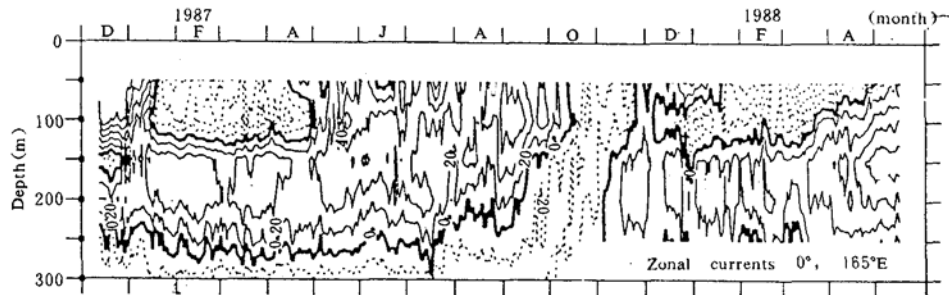


Fig. 2. Time series of zonal velocity at 0°, 165° E from mooring data (provided by Dr. McPhaden).

westward pressure gradient force (or previous westerlies) lagged behind from middle layer to the surface, this phenomenon was similar to the result observed at 0°, 110° W during 1983/1983 EN-SO event by Halpern (1983, 1987). That means that the westward pressure gradient force is of advantage for development of the EIC, and the eastward EUC and surface current turning to westward need an adjusting process (for detail see Section 3).

The local characteristics of the EUC reversion have been discussed above. The spatial variation of the EUC will be analyzed in the following. Figure 3 shows average velocity vectors from 175 m to 225 m layer obtained from ADCP. It can be seen from Fig. 3 that the reverse phenomenon for the EUC occurs near the equator east of 156° E, its east boundary is limited to the east of 165° E; but the eastward EUC just occupies the west of 156° E.

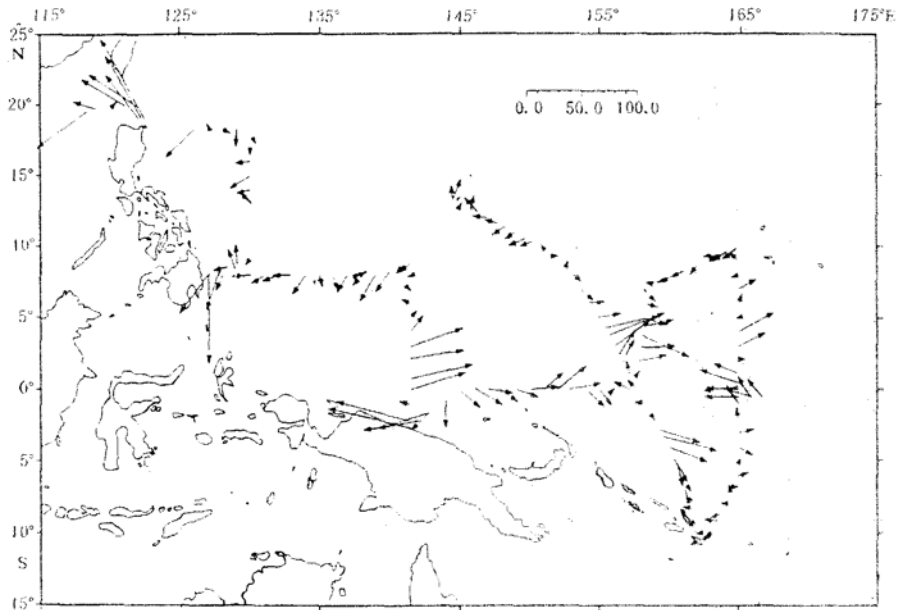


Fig. 3. Average velocity vectors from 175 m to 225 m layers from ADCP data (September 23 – October 26, 1987).

ANALYSIS OF THE EUC REVERSION

In the above section, the evidence for the EUC reversion during 1986/1987 ENSO event and its spatial and temporal variations have been demonstrated. The question is what is the reason for inducing such anomalous phenomenon? We intend to make analysis from the following aspects.

Winds

Time series of zonal winds from the equatorial current meter mooring (0° , 165° E) and from Nauru ($0^\circ 34'S$, $166^\circ 55'E$) (see Fig. 4a) show that the easterly winds were much stronger than normal for the first 4 months of 1986, after a 10-d westerly winds burst in May, tradewinds began to relax in the end of June, and were further weakened from July, but anomalous westerlies frequently appeared, and the 50-d strongest westerly winds were measured from the middle of November to the first of January of the ensuing year with typically maximum speed of 10 m/s, then, intermittent westerlies continuously occurred from February to October 1987, during which intense westerly winds persisted for about 60 d. It was thought that these westerlies might be an important factor to trigger ENSO event. After two months westerlies outbreaks (September – October), one month westerly winds were observed in December. The tradewinds were reestablished after February 1988, that marked the end of 1986/1987 ENSO event. If the comparison of Fig. 4a and Fig. 2 is made, it will be easy to find that: (1) the eastward equatorial surface current has time lag relationship with local strong westerlies, but the strength of the subsurface EUC is independent of local westerlies, (2) the EUC responds to strong westerly winds with time

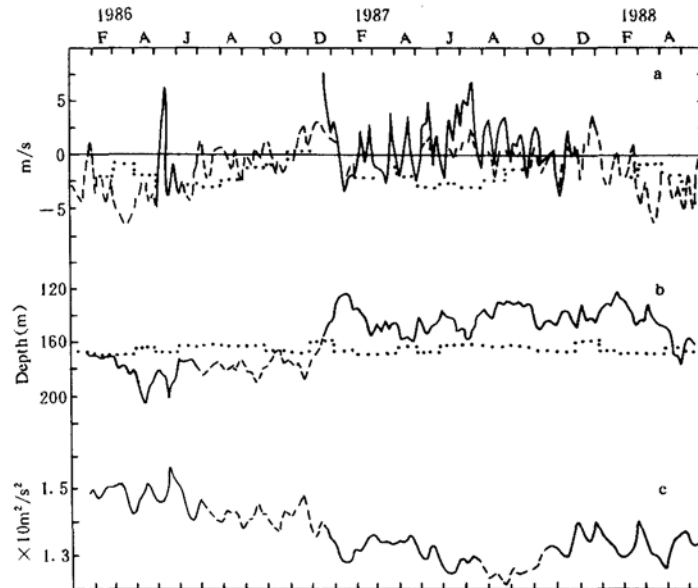


Fig. 4. Time series of (a) winds from equatorial current meter mooring (solid line) and Nauru (dashed line), (b) 20 °C isotherm depth from the equator (solid line) and from 2° N (dashed line) and (c) gravitational potential $0/500 \times 10^2$ hPa from the equator (solid line) and from 2° N (dashed line) (cited McPhaden, 1990).

lag of about 40 d.

The depth of thermocline and surface gravitational potential

The depth of thermocline and surface gravitational potential from current meter mooring.

Figures 4b and c show the time series of 20 °C isotherm depth which shows the core position of thermocline and surface gravitational potential measured from mooring (0°, 165° E). It can be seen from Fig. 4b that the 20 °C isotherm depth shoaled extensively at the time behind the occurrence of strong westerlies (during November – December 1986) by about one and half months; and the variation of surface gravitational potential ($0/500 \times 10^2$ hPa) is opposite from that of thermocline and surface zonal winds, its minimum value appeared in the end of August 1987. That reflects the large scale Euler variation in the surface.

Surface zonal gradient along the equator

The zonal pressure gradient force is characterized by the surface zonal gradient. Wyrtki (1984) noted from surface gravitational potential relative to 500×10^2 hPa near the equator (1° S ~ 1° N) estimated from thermohaline historical data that the sea surface general situation in the equatorial area of the Pacific is high in the west and low in the east, the mean gradient of sea level is about -3×10^{-8} . Owing to pronounced difference in winds and thermal conditions at the equator, the highest sea level appears near 160° E with thick warm water accumulated, and the sea

level slightly slopes down west of 160° E, reaches lowest at about 100° W where cold upwelling prevails, the sea level slope is about -4×10^{-8} and -6×10^{-8} at 160° E~ 140° W and 140° ~ 100° W respectively. The difference of sea level slope between the east and the west is coherent with zonal variation of sea surface wind stress. That is, southeast tradewinds accelerate westward between 140° and 100° W; and decelerate between 160° E and 140° W, westerlies often appear west of 150° E because of the influence of East Asia monsoon and cross-equatorial flow in the Southern Hemisphere.

During the ENSO event, with the collapse of the above wind condition, eastward stretching of westerlies and eastward transport of the upper warm water, the spike of sea level in near 160° E gradually moves eastward that brings about the following results (Wang *et al.*, 1988, 1989; Wyrski, 1984):

(1) It is seen from Fig. 4c that the sea level drops in fixed position and in certain period of time.

(2) the westward pressure gradient force forms west of sea level peak as the sea surface

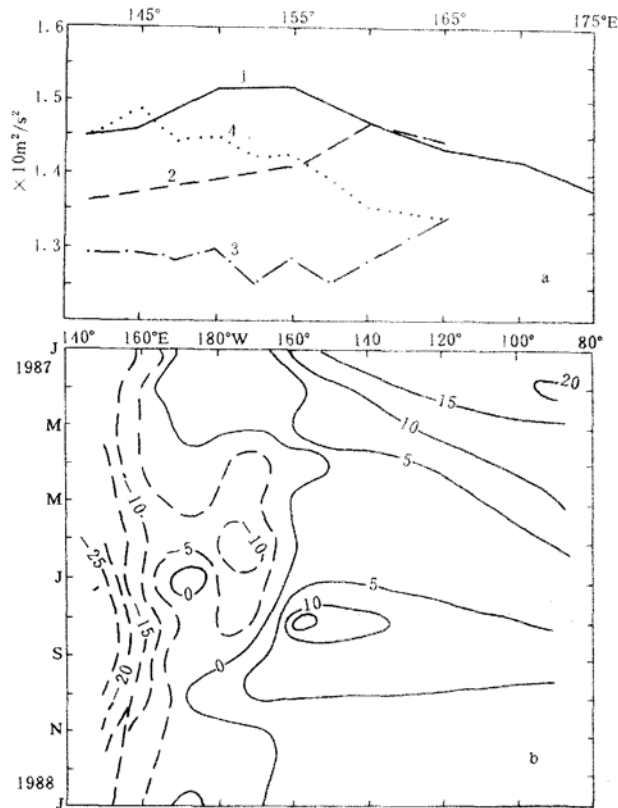


Fig. 5. Distribution of gravitational potential $\phi/500 \times 10^2$ hPa from 4 equatorial sections: 1. first cruise (January 12 - February 10, 1986), 2. second cruise (November 30 - December 11, 1986), 3. third cruise (October 3~17, 1987) and 4. fourth cruise (May 5~20, 1988) (a) and spatial and temporal variations of the sea level anomalies at the equator (b).

slopes down (Fig. 5). Sea level in Kapingamarangi ($1^{\circ}6'N$, $154^{\circ}47'E$) and Nauru ($0^{\circ}34'S$, $166^{\circ}55'E$) declined westward during the period of June – November 1987, with large drop in September (13×10^{-8}). These imply that the pressure gradient force not only directs towards west but also reaches large value between 155° and $167^{\circ} E$ near the equator. This characteristic is not directly related to local winds condition, but is associated with the strong westerly winds before September (see Fig. 4a). It is noteworthy that the above phenomenon appeared not only in this ENSO event, actually, Guan (1986) and Firing *et al.* (1983) found that of the upper and middle parts the EUC entirely disappeared at $137^{\circ} E$ (in the beginning of July 1982) and 0° , $159^{\circ} W$ (during September – December 1982) respectively, all these phenomena were caused by the sea level westward drop (they were 8×10^{-8} and $4 \times 13 \times 10^{-8}$ respectively) (Guan, 1986; Wyrki, 1984); Halpern (1983, 1987) discovered the evidence of the EUC reversion, although there is no pressure gradient force data to prove the fact, yet it is clearly indicated that this anomalous phenomenon is not related to local winds.

In addition, the vertical distribution of zonal pressure gradient force relative to 500×10^2 hPa estimated from CTD data (Mangum *et al.*, 1990) (Fig. 6) shows that there was westward pressure gradient force in the water layer shallower than 325 m except for the layer between 25 and

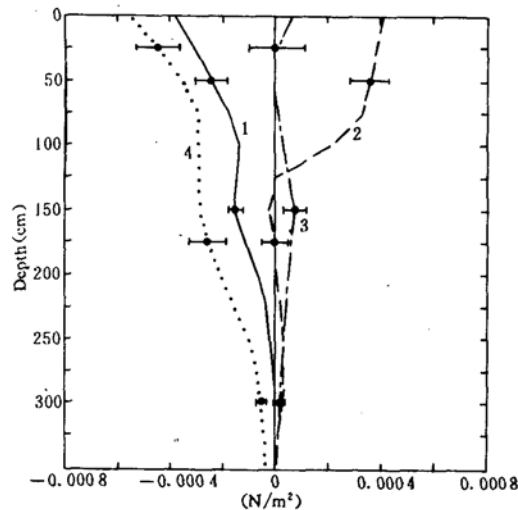


Fig. 6. Vertical distribution of pressure gradient force relative to 500×10^2 hPa along the equator. 1. First cruise, 2. second cruise, 3. third cruise and 4. fourth cruise. (cited Mangum *et al.*, 1990)

65 m where pressure gradient force approached to zero during the EUC reverse period (September – October, 1987).

It is clarified from the above-mentioned facts that the inversion of the EUC is related to westward pressure gradient force. meanwhile, the latter is favourable to the EIC in development and expansion. Because the EUC needs certain adjusting process when switching from eastward

to westward flowing, the EIC response to westward pressure gradient force prior to the EUC (see Fig. 2).

THE SIMULATION OF THE EUC REVERSION

It has been pointed out from theoretical studies that the necessary condition for the formation of the EUC is eastward pressure gradient force which responds to eastward tradewinds (Gill, 1982; Philander, 1980; Philander and Pacanowski, 1980). The above analysis confirms that permanent intense westerlies will induce eastward pressure gradient force to westward, so that it results in partial and entire reverse flowing of the EUC during ENSO event.

In order to verify the above analysis, a numerical model is constructed as follows.

Governing equations

In Cartesian coordinate systems, undisturbed plane is taken as xoy plane, and x , y and z axes represent eastward, northward and upperward directions respectively, the principal equation can be written as following form:

$$\frac{\partial u}{\partial t} + u \frac{\partial u}{\partial x} + v \frac{\partial u}{\partial y} + w \frac{\partial u}{\partial z} - \beta y v = -\frac{1}{\rho_w} \frac{\partial P}{\partial x} + \mu \frac{\partial^2 u}{\partial z^2}, \quad (1)$$

$$\frac{\partial v}{\partial t} + u \frac{\partial v}{\partial x} + v \frac{\partial v}{\partial y} + w \frac{\partial v}{\partial z} + \beta y u = -\frac{1}{\rho_w} \frac{\partial P}{\partial y} + \mu \frac{\partial^2 v}{\partial z^2}, \quad (2)$$

$$\frac{\partial u}{\partial x} + \frac{\partial v}{\partial y} + \frac{\partial w}{\partial z} = 0, \quad (3)$$

where u , v and w denote the velocity components in x , y and z directions respectively, $\beta = f/y$, f the Coriolis parameter, P the pressure, μ the vertical turbulent viscosity coefficient. Assuming velocity components u and v independent of x near the equator, Eqs (1) ~ (3) can be transferred into

$$\frac{\partial u}{\partial t} + v \frac{\partial u}{\partial y} + w \frac{\partial u}{\partial z} - \beta y v = -\frac{1}{\rho_w} \frac{\partial P}{\partial x} + \mu \frac{\partial^2 u}{\partial z^2}, \quad (4)$$

$$\frac{\partial v}{\partial t} + v \frac{\partial v}{\partial y} + w \frac{\partial v}{\partial z} + \beta y u = -\frac{1}{\rho_w} \frac{\partial P}{\partial y} + \mu \frac{\partial^2 v}{\partial z^2}, \quad (5)$$

$$\frac{\partial v}{\partial y} + \frac{\partial w}{\partial z} = 0. \quad (6)$$

Equations (4) ~ (6) are known as "cross section" model (Charney, 1960; Mihailova *et al.*, 1975).

For the convenience of solving Eqs (4) ~ (6), first of all, making derivative of Eq. (5) with respect to y , then integrating Eq. (6) over z , we get

$$\frac{\partial w}{\partial t} + \int_0^z v \frac{\partial^2 v}{\partial y \partial z} + w \frac{\partial^2 w}{\partial z^2} - \left(\frac{\partial w}{\partial z}\right)^2 - \frac{\partial w}{\partial y} \frac{\partial v}{\partial z} - \beta u - \beta y \frac{\partial u}{\partial y} - \frac{1}{\rho_w} \frac{\partial^2 P}{\partial y^2} dz = \mu \frac{\partial^2 w}{\partial z^2}. \quad (7)$$

Equations (4), (5) and (7) are regarded as the governing equations.

De finite condition

Solving boundary condition:

$$\begin{aligned}
 \mu \frac{\partial u}{\partial z} &= -\tau_x, \quad \mu \frac{\partial v}{\partial z} = 0, \quad w = 0 && \text{at upper boundary,} \\
 u = v = w &= 0 && \text{at lower boundary,} \\
 \frac{\partial u}{\partial y} = \frac{\partial v}{\partial y} = \frac{\partial w}{\partial z} &= 0 && \text{at lateral boundary,} \\
 u = v = w &= 0 && \text{when } t = t_0.
 \end{aligned}$$

Solution

Taking $\Delta y = 50$ km and $\Delta z = 30$ m on meridional profile; and making the southern and northern boundary of the profile symmetrical to the equator with the length of 800 km; taking the lower layer of thermocline as lower boundary of the profile, i. e. $H = 300$ m, in the meantime, liquid bottom (the sea water below the liquid bottom is homogeneous) is assumed. The zonal wind is only considered in the wind field, and its meridional variation presenting in the following is inhomogeneous: $w_{10S} = 9/16(j-1)$ and $w_{10N} = -3 + 3/4(33-j)$ represents the wind variation in the southern and northern parts of the equator, in which j denotes the number of meridional grid (Fig. 7). This wind field demonstrates permanent strong westerly winds during 1986/1987 EN-SO event.

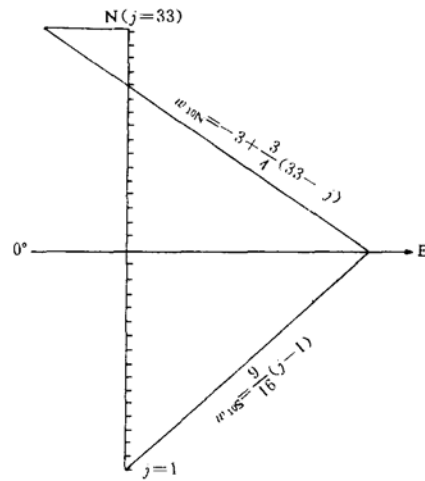


Fig. 7. Meridional structure of simulated wind field.

The relevant parameter values in calculation are specified as follows:

$$\begin{aligned}
 \mu &= 20 \text{ cm}^2/\text{s}, \quad \tau_x = \rho_a \cdot C_D \cdot w_{10}^2, \quad \rho_a = 1.229 \cdot 10^{-3} \text{ g/cm}^3, \\
 C_D &= (0.8719 + 0.000704w_{10}) \cdot 10^{-3}, \quad (w_{10}: \text{cm/s})
 \end{aligned}$$

$$\frac{1}{\rho_w} \frac{\partial P}{\partial x} = \frac{\tau_x}{\rho_w H}, \quad \rho_w = 1.024 \text{ g/cm}^3.$$

The results of simulation and discussions

The results for simulation are drawn in Fig. 8. It can be seen from Fig. 8a that the

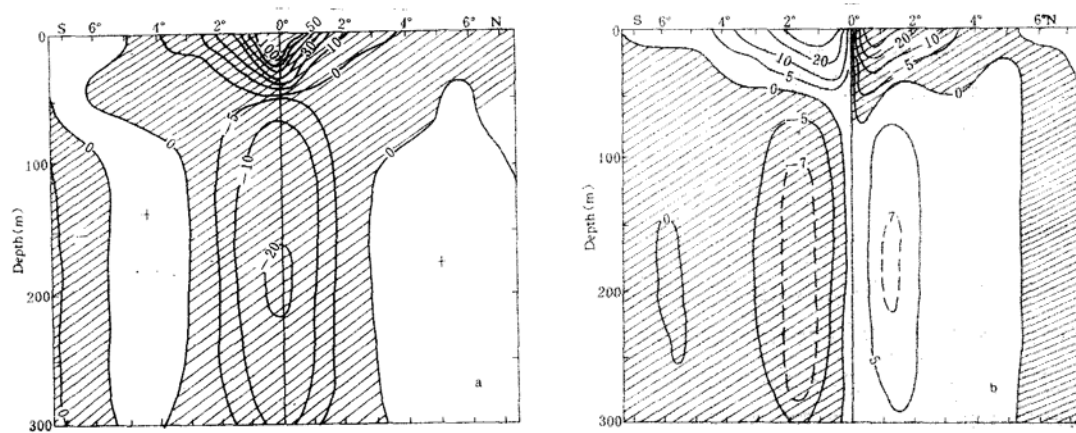


Fig. 8. Simulated velocity components u (a) and v (b) profiles.

strongest eastward jet appears on the upper layer near the equator, with the maximum speed of about 130 cm/s. This result is consistent with that observed from the second cruise (November–December, 1986) of PRC/USA joint air-sea interaction studies in the western tropical Pacific (Wang *et al.*, 1988, 1989). The reverse flowing of the EUC occurs below the upper eastward equatorial current (EEC) with its range between 3° S and 3° N, its core position is situated at 200 m. At the same time, the South and North Equatorial Counter-current (SECC, NECC) south and north of the equator weakens, the pattern and tendency of this current field are very similar to those in Fig. 1. Figure 8b shows simulated northward velocity component profile, it presents that there is intense convergence in the area shallower than 50 m near the equator, that makes upper isotherm near the equator concave (see Fig. 9a). But in the depth deeper than 50 m, there occurs stronger divergence, consequently, with the development of the EUC, the peculiar rhombic structure disappears in the thermocline near the equator, and stretching and thickening thermocline appears instead (see Fig. 9b).

CONCLUSIONS

Through the above analysis and numerical simulation, the following results can be concluded:

1. The direct cause for the reverse flowing of the EUC is related to reversal of pressure gradient force, and the latter is influenced by permanent westerlies in the previous period of ENSO, and it is independent of local winds.

2. The reversion of the EUC makes an impact on thermocline and anomalous distributions of its inner physical, chemical and biological characteristics (the latter two terms are omitted here, for detail, see Chapter 5 of *Comprehensive Study of the Air-sea Interaction Studies in the Western Tropical Pacific*).

3. Although only a few evidences for the reversion of the EUC have been observed interna-

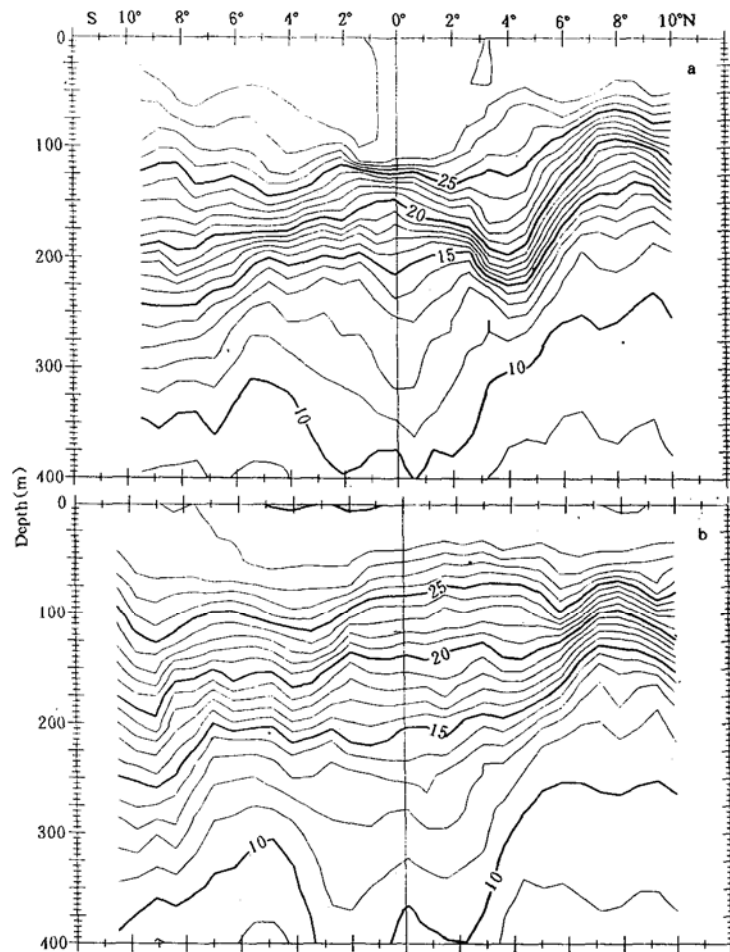


Fig. 9. Temperature profiles along 165° E section for (a) the westerlies burst period of ENSO (November, 1986) and (b) reverse period of the Equatorial Undercurrent (October, 1987).

tionally so far, however, the westward pressure gradient force frequently forms west of warm water dome during eastward the warm water transport in the western Pacific eastward in each ENSO event. It can be inferred that the phenomenon for the EUC partial or entire reversion occurs at times during ENSO event.

REFERENCES

- Charney J. G. (1960) Nonlinear theory of a wind-driven homogeneous layer near the equator. *Deep-Sea Research*, **6** (4), 372~381.
- Firing E. *et al.* (1983) Equatorial Undercurrent disappears during 1982/1983 El Niño. *Science*, **222**, 1121~1123.
- Gill A. E. (1982) *Atmosphere-Ocean Dynamics* (Chapter 11): The tropical zone, Academic Press, 337~380.
- Guan Bingxian (1986) Current structure and its variation in the equatorial area of the western North Pacific Ocean. *Chinese J.*

- Oceanol. Limnol.*, **4**(3), 239~255.
- Halpern D. (1983) Variability of the Cromwell Current at 110° W before and during the 1982/1983 warm event. *Trop. Ocean Atmos. Newsletter*, **21**, 9~11.
- Halpern D. (1987) Observations of annual and El Niño thermal and flow variations at 0°, 110° W and 0°, 95° W during 1980~1985. *J. Geophys. Res.*, **92** (C8), 8197~8212.
- Mangum L. J. *et al.* (1990) The zonal pressure gradient in the western equatorial Pacific Ocean. *J. Geophys. Res.*, **95** (C5), 7279~7288.
- McCreary J. P. (1981) A linear stratified ocean model of the Equatorial Undercurrent. *Philos. Trans. R. Soc. London, Ser. A***298**, 603~635.
- McPhaden M. J. *et al.* (1990) Variability in the western equatorial Pacific Ocean during the 1986/1987 El Niño/Southern Oscillation event. *J. Phys. Oceanogr.*, **20**, 190~208.
- Mikhailova E. N. *et al.* (1975) Wind non-uniformity effects upon the equatorial currents. *Oceanology* (in Russian), **15** (4), 574~579.
- Picaut J. and R. Tournier (1988) Transport variability of the equatorial current in the western Pacific Ocean during 1979~1985. In: *Proceedings of US-PRC Intern. TOGA Sympos.*, China Ocean Press, Beijing, pp. 153~165.
- Philander S. G. H. (1980) The Equatorial Undercurrent revisited. *Ann. Rev. Earth Planet. Sci.*, **8**, 191~204.
- Philander S. G. H. and R. C. Pacanowski (1980) The generation of equatorial currents. *J. Geophys. Res.*, **85**, 1123~1185.
- State Oceanic Administration of PRC (1981) (edited by Wang Zongshan) *Xiangyanghong 09 Observational Report of the Western Central Pacific* (in Chinese), China Ocean Press, Beijing, pp. 40~69.
- Wang Zongshan and Zou Emei (1987) Current variations in the western tropical Pacific Ocean. *Huanghai and Bohai Seas* (in Chinese), **5** (2), 17~27.
- Wang Zongshan *et al.* (1988) Oceanic event during the 1986/1987 El Niño. In: *Proceedings of US-PRC Intern. TOGA Sympos.*, China Ocean Press, Beijing, pp. 15~26.
- Wang Zongshan *et al.* (1989) The response of water masses and Equatorial Undercurrent in the western Pacific Ocean to the 1988/1987 El Niño event. *TOGA Sci. Conference, July 16~20*, Honolulu, 18pp.
- Wyrtki K. (1984) The slope of sea level along the equator during the 1982/1983 El Niño. *J. Geophys. Res.*, **89** (C6), 10419~10424.